BULLETIN OF THE POLISH ACADEMY OF SCIENCES
TECHNICAL SCIENCES, Vol. 68, No. 3, 2020
DOI: 10.24425/bpasts.2020.133381

Determination of hazardous metal ions in the water with resonant MEMS biosensor frequency shift – concept and preliminary theoretical analysis

Z. RAHIMI[1*], J. YAZDANI[2], H. HATAMI[3], W. SUMELKA[4], D. BALEANU[5,6], and S. NAJAFI[1]

[1] Department of Mechanical Engineering, Urmia University, Urmia, Iran
[2] Department of Geology, Lorestan University, Khorramabad, Iran
[3] Department of Mechanical Engineering, University of Guilan, Rasht, Iran
[4] Institute of Structural Engineering, Poznan University of Technology, Piotrowo 5 Street, 60-965 Poznan, Poland
[5] Department of Mathematics, Cankaya University, Ankara, Turkey
[6] Institute of Space Sciences, Magurele, Romania

Abstract. Heavy metal ions (e.g. cadmium, chromium, copper, nickel, arsenic, lead, zinc) have significantly serious side effects on the human health. They can bind with proteins and enzymes, altering their activity, increasing neurotoxicity, generating reactive oxygen species (ROS), promote cellular stress and resulting in their damage. Furthermore, the size, shape and type of metal are important for considering nano- or microtoxicity. It then becomes clear that the levels of these metals in drinking water are an important issue. Herein, a new micro-mechanical sensor is proposed to detect and measure these hazardous metals. The sensor consists of a micro-beam inside a micro-container. The surface of the beam is coated with a specific protein that may bind heavy metals. The mass adsorbed is measured using the resonant frequency shift of the micro-beam. This frequency shift due to the admissible mass (which is considered acceptable for drinking water based on the World Health Organization (WHO) standard) of manganese (Mn), lead (Pb), copper (Cu) and cadmium (Cd) is investigated for the first, second and third mode, respectively. Additionally, the effects of micro-beam off-center positions inside the micro-container and the mass location are investigated.

Key words: micro-mechanical sensor, hazardous metals, resonant frequency shift, micro mass-sensor, drinking water.

1. Introduction

Increasing industrial activities give rise to environmental problems such as heavy or hazardous metals water pollution, which causes the freshwater supply to become one of the most important issues of today's world [1]. In addition, the serious side effects that those heavy metals (including cadmium, chromium, copper, nickel, arsenic, lead and zinc) exert on the human health are significant [2, 3]. For instance, the corruption of the brain and nervous system, behavioral and learning defects, rise of blood pressure, kidney damage and bloodlessness are some of those already recorded [4–6]. As an example, side effects in the respiratory tract and in the brain, temporary gastrointestinal distress with symptoms such as nausea, vomiting, abdominal pain, destruction of red blood cells, damage to the central and peripheral nervous system, learning disabilities, shorter stature, impaired hearing, and impaired formation and function of blood cells are mentioned for manganese, cadmium, lead and copper [7]. These hazardous metals contaminate the groundwater and surface water through a natural process and anthropogenic activities (e.g. fastest-growing industrial zones [leather goods, metal products, dyeing, fertilizers, textiles, chemicals etc.], agriculture, mining and traffic activities). To this end, measuring and monitoring contamination levels of these metals constitute an important and vital issue, which leads to proposing different methods such as atomic adsorption spectrometry and inductively coupled plasma mass spectroscopy [8–10], optical sensors and biosensors [11, 12], or electrochemical methods [13–16]. In the present study, a micro electro mechanical system (MEMS) has been investigated to measure hazardous metals in water. The developed concept of a biosensor can be used in different zones which contain the metals impurities discharged into the natural rivers and dams and eventually permeate through the groundwater that is used for drinking purposes [17–20].

In recent years, micromechanical systems have found widespread use as mass-sensors in different fields of science and engineering [21–27] due to high sensitivity, short response time, specificity and relatively low cost of production [28]. One of the approaches of mass identification is based on a resonant frequency shift while carrying a target entity [29] where the resonant frequency is measured before and after mass adhesion/adsorption to the surface of the micro-beam. The difference between these two frequencies enables us to measure the mass of pollution. Resonant mass sensors, especially of the can-

*e-mail: st_z.rahimi@urmia.ac.ir

Manuscript submitted 2019-08-02, revised 2020-02-18, initially accepted for publication 2020-02-02, published in June 2020

tilever type, have been utilized to quantify the mass of bacteria and viruses [30, 31]. Characterization mass of single live cells in fluids [32] mass of a single-stranded DNA [33] and their application as a diagnostic assay for the protein markers of prostate cancer [34] have been reported. A new class of plant metal-binding proteins has also been described [35]. They are capable of binding multiple atoms of different heavy metals. Nevertheless, there are groups of metal-binding proteins with the capability of selective blinding to adsorb a specific heavy metal [36, 37].

In this study, we presented a new micromechanical sensor to characterize hazardous metals in water – both the concept and its mathematical model. The micro sensor consists of a micro-cantilever located inside a micro space (micro-container). The micro-container fills up with water samples throughout a series of micro-channels and then the metal ion is to be adsorbed onto the surface of the beam (which is coated with specific proteins) – the mass of that ions is be measured. The protein is located on a layer of gold [36, 37]. It should be pointed out that there are different materials which are able to indicate particular heavy metals in drinking water. They include synthetic receptors and siological receptors where among them antibodies offer significant advantages over traditional detection methods, such as high sensitivity, selectivity and species-specificity. Therefore, the protein constitutes the case study explaining our model [38]. Repeat proteins could be used as an example, due to their highly stable molecules – the array of protein tandem repeats have clearly higher thermodynamic stability than the one reported for natural biomolecules (protein), considering the same length – therefore in the consensus (the designed, well-expressed protein, then synthesized, purified and checked) they present a more folded framework, which makes for higher mechanical or thermal stability. According to Braun et al. [39] and Hara et al. [40], the mass of proteins and gold layers are 0.175 ng and 0.720 ng, respectively. Furthermore, cavitation is ignored – Kapustina [41] thoroughly analyzed ultrasonic degassing mechanisms in water and concluded that the oscillations of the bubbles in the acoustic field play the most important role, while ultrasonic cavitation takes the supportive role in intensifying bubble formation and accelerating bubble/liquid interfacial diffusion. Finally, the mass of the heavy metal adsorbed causes a shift in the resonant frequency of the micro-beam and, consequently, someone can measure the mass of the heavy metals using the frequency shift. It is important that micro and nano-sensors can sense the small changes in harmful metal levels easily and more effectively, so micromechanical sensors are suitable for this purpose [17–20].

The micro-sensor is modeled as a micro-beam resonator submerged in a bounded incompressible fluid domain with a lumped mass on the surface of the beam. Finally, we investigate the frequency shift caused by the adsorbed mass of Mn, Pb, Cu and Cd. The lumped mass has been considered in a situation where majority of the adsorbed metals concentrate in a particular location. This occurs in a situation where just a part of the beam is coated with gold; therefore, only that part acts as a metals receptor. On the other hand, if the protein layer does not spread uniformly, the concentration of the metals might be larger in that part and as an assumption it has been considered that the mass of metals on other side is neglected. In addition, we show the effects of different parameters, such as the off-center positions of the micro-beam inside the micro space, positions of the adsorbed mass and ratio of the adsorbed mass to beam mass on the first, second and third resonant frequencies.

It should be noted that the proposed micromechanical sensor and its characterization for monitoring hazardous metals in drinking water have been investigated for the first time. In addition, the form of the proposed mathematical model of the micro resonator submerged in a bounded incompressible fluid domain with a lumped mass on the surface is yet another novelty of this paper. The modeling is mass-location sensitive – in other words, it could characterize different mass locations.

2. Micro-sensor proposed

A schematic view of the micro-sensor has been shown in Fig. 1. As can be seen, the proposed sensor consists of a micro-beam inside a micro-container. The micro-beam is made of silicon nitride and gold-coated on one side [42] and additionally functioned with proteins that can bind multiple atoms of hazardous metals [35]. The micro-container is filled up with a water sample. A drop of the sample thrown onto a pad through the micro-channels is transferred to the inside of the container space.

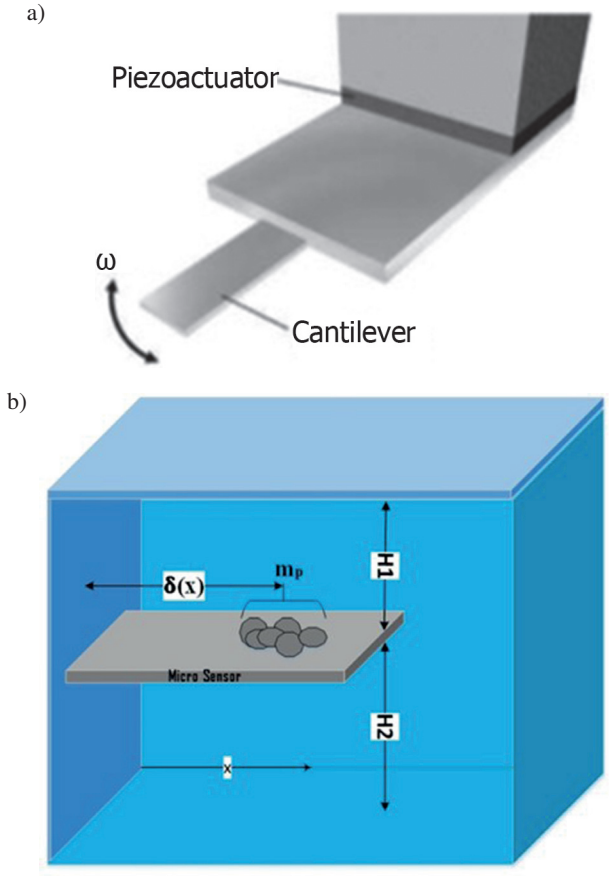

Fig. 1. a) Harmonic vibration-type micro-cantilever sensor using a piezo actuator [45]; b) Schematic view of proposed micro-sensor

When the ions of hazardous metal are adsorbed to the surface of the beam, the effect on the resonant frequency of the micro-beam causes its shift. Characterization of the shift values leads to measuring the amount of pollution (mp). The frequency of the micro-sensor could be measured via different methods, such as the laser Doppler vibrometer (LDV) [43, 44]. Physical parameters of the micro-sensor are: container length, $a = 350$ μm, container height, $H = 600$ μm, micro-beam length $L = 25$ μm, micro-beam width, $b = 50$ μm, micro-beam thickness, $h = 3$ μm, liquid depth of upper and lower domains $H_1 = H_2 = 300$ μm, micro-beam Young's modulus, $E = 192$ GPs, mass of micro-beam per unit length $\rho_b = 3.4965 \times 10^{-7}$ kg/m, fluid density $\rho_f = 1000$ kg/m^3, and Poisson's ratio, $\vartheta = 0.28$.

3. Mathematical modeling and solution

As mentioned above, one side of the micro-beam is coated with gold. The thickness of the gold is ignorable in comparison to the micro-beam thickness; therefore, the equation of motion for free small lateral vibration of the micro-beam interacting with the surrounding fluid is [46]:

$$EI\frac{\partial^4 w}{\partial x^4} + \rho_{ef}\frac{\partial^2 w}{\partial t^2} = b(P_1 - P_2) \tag{1}$$

where EI is the bending stiffness of the micro-beam, ρ_{ef} is the total length density of the protein, gold layer and beam, which represents the hydrodynamic pressures imposed by fluid oscillation in the lower and upper regions. Herein, the adsorbed ions of hazardous metals are considered as a lumped mass (m_p) which is located in distant $\delta(x)$. Considering m_p, the equation of the motion will be [47]:

$$\begin{aligned} EI\frac{\partial^4 w(x,t)}{\partial x^4} + \rho_{ef}\frac{\partial^2 w(x,t)}{\partial t^2} + m_p\frac{\partial^2 w(x,t)}{\partial t^2}\delta(x-\delta) \\ = b(P_1 - P_2) \end{aligned} \tag{2}$$

where the hydrodynamic pressures are [48, 49]:

$$P_1 = -\rho_f \left.\frac{\partial \eta_1}{\partial t}\right|_{y_1=H_1}, \qquad P_2 = -\rho_f \left.\frac{\partial \eta_2}{\partial t}\right|_{y_2=0} \tag{3}$$

where $\eta_1(x)$ and $\eta_2(x)$ are the velocity potential functions of the fluids in domains one and two. Functions $\eta_1(x)$ and $\eta_2(x)$ are [50]:

$$\eta_1(x,y_1,t) = \sum_{i=1}^{\infty} A_i(t)(\cos\lambda_i x)(\cosh\beta_i y_1), \tag{4}$$

$$\begin{aligned} \eta_2(x,y_2,t) = \sum_{i=1}^{\infty} E_i(t)(\cos\lambda_i x)\times \\ [(\cosh\gamma_i y_2) - H_2(\tanh\gamma_i)(\sinh\gamma_i y_2)] \end{aligned} \tag{5}$$

where $\lambda_i = (i\pi/a)$, $\beta_i = (i\pi H_1/a)$, $\gamma_i = (i\pi H_2/a)$, $E_i(t)$ and $A_i(t)$ are the undisclosed modal amplitudes for fluid oscillation.

Boundary conditions of fluid movement in both regions (upper and lower) lead to the following equations, respectively:

$$\left.\frac{\partial \eta_1}{\partial y_1}\right|_{y_1=H_2} = \begin{cases} \dfrac{\partial w}{\partial t} & 0 < x < l, \\ \left.\dfrac{\partial \eta_2}{\partial y_2}\right|_{y_2=0} & l < x < a; \end{cases} \tag{6}$$

$$\left.\frac{\partial \eta_2}{\partial y_2}\right|_{y_2=0} = \begin{cases} \dfrac{\partial w}{\partial t} & 0 < x < l, \\ \left.\dfrac{\partial \eta_1}{\partial y_1}\right|_{y_1=H_2} & l < x < a. \end{cases} \tag{7}$$

Using the Galerkin method, the transverse displacement of the beam is approximated as below [51, 52]:

$$w(x,t) = \sum_{i=1}^{\infty} q_i(t)\varphi_i(x) \tag{8}$$

where $\varphi(x)$ is a shape function of the micro-beam in the absence of the fluid (cf. [49]) and $q_i(t)$ is a time-dependent function. Since the highest derivative of w with respect to x and t is two, specifying four boundary conditions and two initial conditions will be needed to finding solution $w(x,t)$ [53]. Substituting Eq. (8) into Eq. (1) and also Eq. (4), Eq. (5) and Eq. (8) into Eq. (6) and Eq. (7) leads to the three equations as below:

$$\begin{aligned} EI\sum_{i=1}^{\infty} q_i(t)\varphi_i^{IV}(x) + \rho_{ef}\sum_{i=1}^{\infty}\ddot{q}_i(t)\varphi_i(x) + \\ + m_p\sum_{i=1}^{\infty}\ddot{q}_i(t)\varphi_i(x)\delta(x-\delta) = \\ = -b\rho_f\left[\sum_{i=1}^{\infty}\dot{A}_i(t)(\cos\lambda_i x)(\cosh\beta_i y_1 \right. \\ \left. - \sum_{i=1}^{\infty} E_i(t)(\cos\lambda_i x)\right], \end{aligned} \tag{9}$$

$$\begin{aligned} \sum_{i=1}^{\infty} A_i(t)H_1\lambda_i(\cos\lambda_i x)(\sinh\beta_i) = \\ = \begin{cases} \displaystyle\sum_{i=1}^{\infty} q_i(t)\varphi_i(x) & 0 < x < l \\ \displaystyle\sum_{i=1}^{\infty} E_i(t)\gamma_i(\cos\gamma_i x)\big[-H_2(\tanh\gamma_i)\big] & l < x < a, \end{cases} \end{aligned} \tag{10}$$

$$\begin{aligned} -\sum_{i=1}^{\infty} E_i(t)\gamma_i H_2(\cos\gamma_i x)(\tanh\gamma_i) = \\ = \begin{cases} \displaystyle\sum_{i=1}^{\infty} q_i(t)\varphi_i(x) & 0 < x < l, \\ \displaystyle\sum_{i=1}^{\infty} A_i(t)\lambda_i(\cos\lambda_i x)(\sinh\beta_i y_1) & l < x < a. \end{cases} \end{aligned} \tag{11}$$

Using the orthogonal property of the mode shapes, both sides of the above equations are multiplied by φ_j and then integrated

over 0 to L, and therefore the following equations are obtained:

$$EI\int_0^L \varphi_i^{IV}(x)\varphi_j(x)q_i(t)+\rho_{ef}\int_0^L \varphi_i(x)\varphi_j(x)\ddot{q}_i(t)+ +m_p\int_0^L \varphi_i(x)\varphi_j(x)\ddot{q}_i(t)\delta(x-\delta)= = -b\rho_f\left[\sum_{i=1}^{\infty}\dot{A}_i(t)\left[\xi_{ij}H_1(\sinh\beta_i)\right]-\sum_{i=1}^{\infty}E_i(t)\xi_{ij}\right], \tag{12}$$

$$\left(\frac{a}{2}\right)\beta_j A_j(t)\left[H_1(\sinh\beta_j)\right]=\sum_{i=1}^{\infty}q_i(t)\xi_{ji} -\sum_{i=1}^{\infty}E_i(t)\gamma_i\chi_{ij}\left[H_2(\tanh\gamma_i)\right], \tag{13}$$

$$-\left(\frac{a}{2}\right)\gamma_j E_j(t)\left[H_2(\tanh\gamma_j)\right]=\sum_{i=1}^{\infty}q_i(t)\xi_{ji} -\sum_{i=1}^{\infty}A_i(t)\beta_i\chi_{ij}\left[H_i(\sinh\beta_i)\right] \tag{14}$$

where

$$\xi_{ji}=\int_0^l(\cos\lambda_j x)\psi_i(x)\,\mathrm{d}x, \qquad \chi_{ij}=\int_l^a(\cos\lambda_j x)(\cos\lambda_i x)\,\mathrm{d}x. \tag{15}$$

Next, considering n and m modes ($i=1,2,\ldots,n$), ($j=1,2,\ldots,m$) for the micro-beam and fluid oscillation, respectively, the following finite set of matrix equations can be formulated:

$$[\alpha]\ A=[\varpi]\ \dot{q}-[\tau]\ E, \tag{16}$$

$$-[\psi]\ E=[\kappa]\ \dot{q}+[\wp]\ A, \tag{17}$$

$$[K]\ q+[M]\ \ddot{q}=[L]\ \dot{A}-[J]\ \dot{E} \tag{18}$$

where

$$\kappa_{ij}=\xi_{ij}, \quad \wp_{ij}=\chi_{ij}\lambda_j, \quad J_{ij}=\xi_{ji}, \quad \varpi_{ij}=H_2H_1^2\xi_{ji},$$
$$\alpha_{ii}=\lambda_i\left(\frac{a}{2}\right)H_1\sinh(\beta_i), \quad \tau_{ij}=\chi_{ij}\gamma_j H_2\tanh(\gamma_j),$$
$$\psi_{ii}=\gamma_i\left(\frac{a}{2}\right)H_2\tanh(\gamma_j), \quad K_{ii}=EI\int_0^L\psi_i(x)\psi_i^{IV}(x)\,\mathrm{d}x,$$
$$M_{ii}=n_f\rho_{ef}\int_0^L\psi_i^2(x)\,\mathrm{d}x+n_f m_p\psi_i^2(L),$$
$$L_{ij}=\zeta_{ji}H_1(\sinh\beta_j) \tag{19}$$

where n_f is a geometry-dependent correction factor ($n_f=0.24$) for rectangular cantilevers) [54]. Substituting A and E into Eq. (19), the equation of motion of the micro-beam in a non-compressible fluid is:

$$[K]\ q+[M+M_1+M_2]\ \ddot{q}=0, \tag{20}$$

$$M_1=\rho_f b[L]\Big(\left[\alpha^{-1}\varpi\right]-\left[\alpha^{-1}\tau\right]\left[\left(\wp\alpha^{-1}\tau-\psi\right)^{-1}\right]\times \times\left[\varpi+\wp\alpha^{-1}\kappa\right]\Big),$$
$$M_2=-\rho_f b[J]\left[\left(\wp\alpha^{-1}\tau-\psi\right)^{-1}\right]\left[\kappa+\wp\alpha^{-1}\kappa\right]. \tag{21}$$

4. Results

As a case study, the proposed micro-sensor has been used to identify some hazardous metals like Mn, Pb, Cu and Cd. The standard limits of these metals concentration (mg/L) extracted from Guidelines for Drinking-Water Quality of the WHO standard [7] have been shown in Table 1.

Table 1
Standard limits of heavy/hazardous metals concentration in drinking water based on WHO standard

Element	Mn	Cu	Pb	Cd
Standard amount (mg/L)	***0.4***	***2***	***0.01***	***0.003***
Standard amount for the micro-container (ng)	8.4×10^{-3}	4.2×10^{-2}	2.1×10^{-4}	6.3×10^{-5}

As it is visible, these data show admissible mg of the heavy/hazardous metal in one liter of the water sample, therefore, it is needed to convert them for the volume of the proposed micro-sensor, which is the volume of the water sample in the micro-container. Therefore, the standard mass limits of different heavy metals in drinking water have been shown in the second row. The mass m_p bigger than the values in the second row of Table 1 shows contaminated water whereas its smaller values are acceptable.

Validation of the mathematical modeling is presented in Table 2. The fundamental frequencies obtained for different micro-beams in water versus those in literature [55] are in acceptable agreement. Note that the validation has been evaluated by considering $m_p=0$.

Table 2
Comparison of fundamental frequencies (Hz) in water $\rho=1000$ Kg/m^3

Aspect ratio L/b	5	3	2	1
Thickness ratio h/b	0.124	0.061	0.061	0.024
Ref [55]	15.63	18.30	42.30	51.93
Present study	15.62	18.82	46.80	57.90

As mentioned above, the sensing principle is based on the measurement of variations of resonant frequencies caused by

(unknown) additional masses located on certain positions of the initial system. To show the functionality of the proposed model, the effects of various physical parameters have been studied on different consecutive modes in the presence of the adsorbed mass.

In Fig. 2(a–c) and Fig. 3(a–c), the first three resonant frequencies (f1, f2, and f3) versus location of the pollution mass of Mn, Cu, Pb and Cd have been illustrated. The values of m_p are considered based on those which were mentioned in Table 1. In other words, in these figures, the effects of admissible adsorbed mass of different heavy metals have been shown on the frequency shift of different modes where the adsorbed mass is located in different positions. Comparing the first (f_1), second (f_2) and third (f_3) modes, it is visible that in the first mode natural frequency decreases when the micro-sensor adsorbs m_p and at the end of the micro-sensor it obtains the minimum value. In the second and third modes, micro-sensor frequency shows almost periodic behavior in the presence of adsorbed mass. Even though in some m_p positions (e.g. $\delta/L = 0.9$) the value of resonant frequency is higher than for condition $(\delta/L = 0)$.

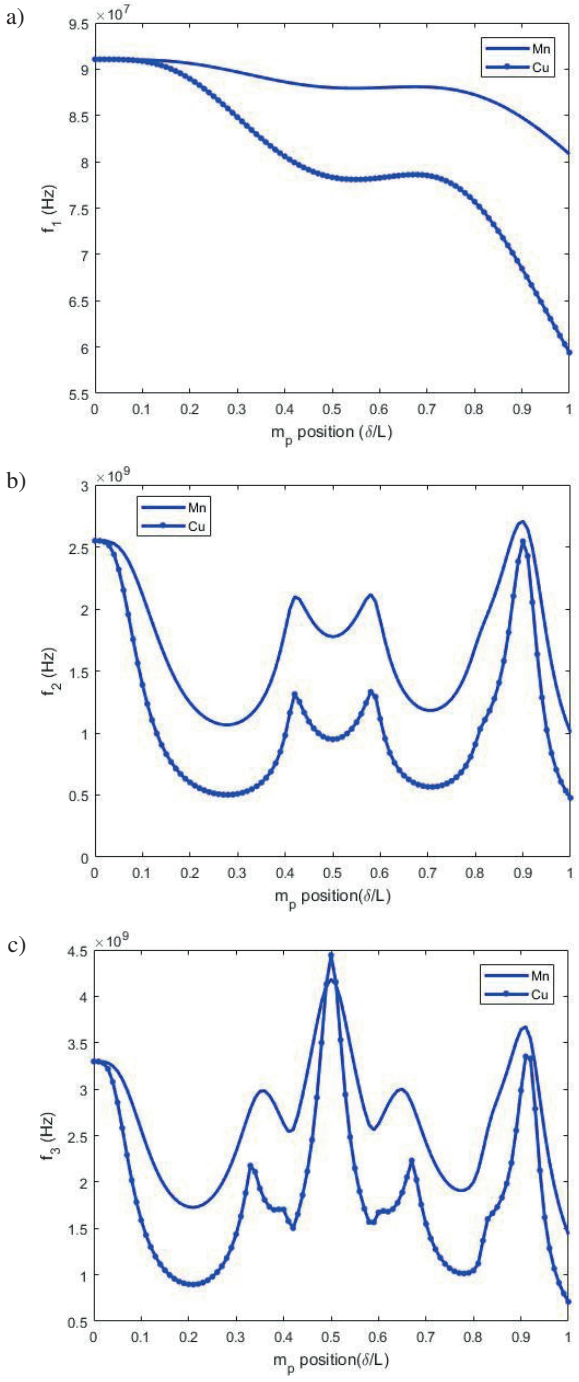

Fig. 2. Variation of the first three resonant frequencies versus different positions of Mn and Cu: a) f_1, b) f_2 and c) f_3

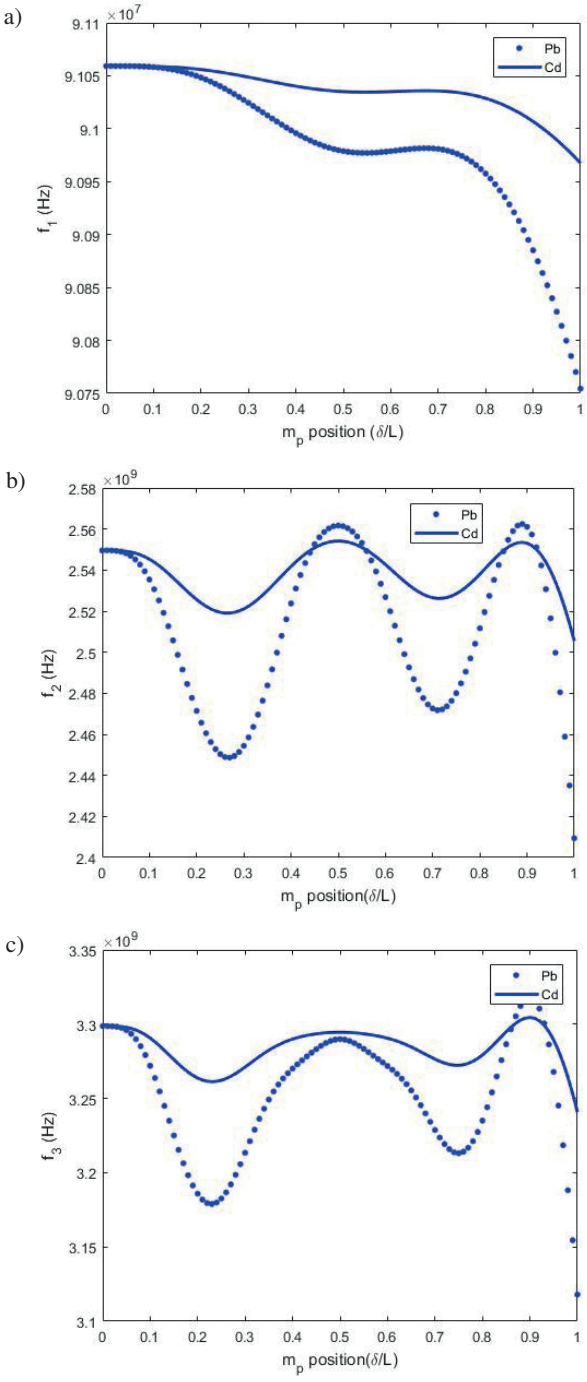

Fig. 3. Variation of resonant frequency versus different positions of Pb and Cd adsorbed mass: a) f_1, b) f_2 and c) f_3

This is apprehensible by considering Eq. (20), (21), where it has been shown that the surrounding fluid movement (due to vibration of the micro-sensor) in the upper and lower domains of the micro-sensor is the external mass added (in opposite direction) to the beam.

Therefore, the additional mass of moving fluid in the lower domain dominates over a summation of the upper fluid and adsorbed mass in those positions. This conclusion is in agreement with the results of Ref. [53].

In Fig. 4, the effects of adsorbed mass variation are illustrated on the first, second and third resonant frequencies of the micro-beam, where the adsorbed mass is located in a different position ($\delta/L = 0.2$, 0.4, 0.6, 0.8 and 1).

This variation is shown for the m_p/m_{ef} ratio, where m_{ef} is the protein, gold layer and micro-beam mass. As can be seen, the rising of the adsorbed mass decreases the resonant frequency of different modes, especially for higher modes. In other words, the higher modes have more sensibility in which this subject is in agreement with those existing in the literature [56]. It means that for higher modes the effects of the adsorbed mass are more significant than for the lower ones.

To propose a complete design of the micro-mechanical sensor, it is needed to show the effects of the micro-beam position inside the micro-container. Therefore, the first, second and third resonant frequencies of the micro-beam with no adsorbed mass are obtained in Table 3 for different values of upper and lower

Table 3
Resonant fundamental frequencies ($\times 10^7$ Hz) of different modes for the micro-beam in water $\rho = 1000$ Kg/m^3 (with no adsorbed mass) where the off-center position has different values

resonant frequency	Off-center position $H_1/(H_1+H_2)$					
	50/600	100/600	150/600	200/600	250/600	300/600
f_1	9.184	8.891	8.983	9.060	9.096	9.106
f_2	249.858	250.206	252.932	254.278	254.816	254.956
f_3	321.230	320.271	324.955	328.055	329.477	329.868

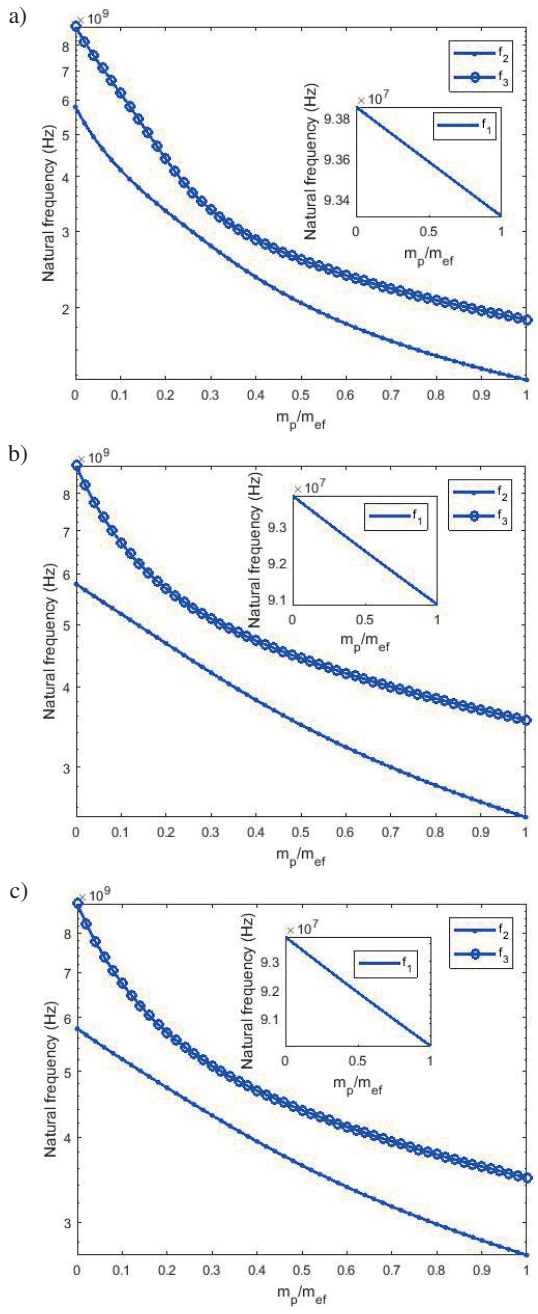

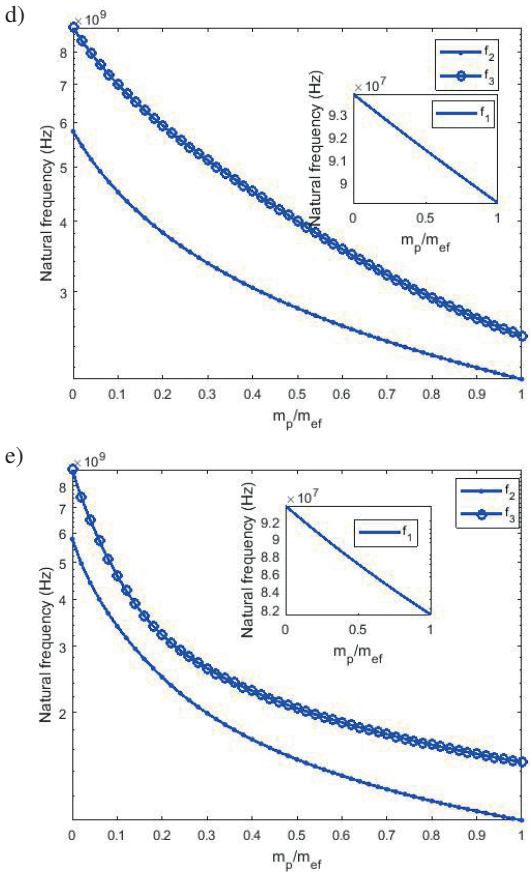

Fig. 4. Variation of resonant frequency versus different ratios of the adsorbed mass to the mass of the protein, gold layer and micro-beam in a different position: a) $\delta/L = 0.2$, b) $\delta/L = 0.4$, c) $\delta/L = 0.6$, d) $\delta/L = 0.8$ and e) $\delta/L = 1$

Table 4
Resonant fundamental frequencies (Hz$\times 10^7$) for the micro-beam in water $\rho = 1000$ Kg/m^3 where admissible Mn mass adsorbed 8.4×10^{-3} ng and off-center position has different values

resonant frequency	Normalized mass location $\delta(x)/L$	Off-center position $H_1/(H_1+H_2)$					
		50/600	100/600	150/600	200/600	250/600	300/600
f_1	0.20	9.14	8.85	8.94	9.02	9.05	9.06
	0.40	8.93	8.66	8.75	8.82	8.85	8.86
	0.60	8.87	8.61	8.69	8.76	8.79	8.80
	0.80	8.79	8.53	8.62	8.68	8.72	8.72
	1.00	8.14	7.93	8.00	8.05	8.08	8.08
f_2	0.20	122.85	122.86	123.60	124.02	124.21	124.26
	0.40	179.80	180.41	181.71	182.42	182.72	182.80
	0.60	187.61	188.08	189.50	190.26	190.58	190.66
	0.80	167.27	167.48	168.59	169.16	169.40	169.46
	1.00	99.68	99.90	100.16	100.30	100.36	100.38
f_3	0.20	172.73	172.71	172.88	172.99	173.04	173.06
	0.40	261.64	261.89	262.33	262.59	262.70	262.73
	0.60	261.25	261.36	261.92	262.26	262.41	262.45
	0.80	197.68	197.52	198.66	199.41	199.76	199.86
	1.00	143.29	143.41	143.51	143.56	143.59	143.59

Table 5
Resonant fundamental frequencies ($\times 10^7$ Hz)) for the micro-beam in water $\rho = 1000$ kg/m^3 where admissible Cd mass adsorbed $m_p = 6.3 \times 10^{-5}$ ng and off-center position have different values

resonant frequency	Normalized mass location $\delta(x)/L$	Off-center position $H_1/(H_1+H_2)$					
		50/600	100/600	150/600	200/600	250/600	300/600
f_1	0.20	9.18	8.89	8.98	9.06	9.10	9.11
	0.40	9.18	8.89	8.98	9.06	9.09	9.10
	0.60	9.18	8.89	8.98	9.06	9.09	9.10
	0.80	9.18	8.89	8.98	9.06	9.09	9.10
	1.00	9.17	8.88	8.97	9.05	9.09	9.10
f_2	0.20	247.44	247.77	250.51	251.87	252.42	252.56
	0.40	249.08	249.43	252.15	253.50	254.04	254.18
	0.60	249.18	249.53	252.25	253.59	254.13	254.27
	0.80	248.75	249.10	251.80	253.13	253.66	253.80
	1.00	245.48	245.82	248.52	249.87	250.41	250.55
f_3	0.20	318.03	317.10	321.61	324.61	325.99	326.37
	0.40	320.53	319.60	324.19	327.22	328.61	329.00
	0.60	320.57	319.63	324.23	327.27	328.67	329.05
	0.80	319.38	318.43	323.06	326.13	327.54	327.93
	1.00	316.01	315.14	319.50	322.39	323.72	324.09

domains. Moreover, in Tables 4 and 5 the effects of the off-center position $H_1/(H_1+H_2)$ have been shown for the low toxic heavy metal (Mn as an example) ions and very toxic elements (Cd as an example). Using Tables 3–5, the effects of admissible adsorbed mass of the hazardous metal ions, its position on the micro-beam and also the position of the micro-beam inside the micro-container on resonant frequencies of the different modes are shown.

5. Conclusion

In this paper, we proposed a new concept of a micro-mechanical sensor to measure hazardous metals in water. It consists of a micro-beam inside a micro-container in which the micro-container fills up with a water sample throughout some micro-channels. The surface of the micro-beam is coated with gold and specific proteins that adsorb specific heavy metals. Resonant frequencies of the micro-beam are shifted by adsorbing the heavy metals and this is the basic concept of the micro-sensor proposed.

Herein, the frequency shift of admissible mass (based on the WHO standard for drinking water) of Mn, Cu, Pb and Cd hazardous metals, the location of the adsorbed mass on the micro-beam as well as effects of different off-center positions of the micro-beam were obtained on the first, second and third resonant frequencies. It was observed that adsorption of the admissible mass of Mn, Cu, Pb and Cd hazardous metals decreased the first, second and third resonant frequencies of the micro-beam. On the other hand, for higher modes, the effects of the adsorbed mass are more significant than for the lower ones.

Acknowledgements. The authors would like to show their gratitude to Professor Ghader Rezazadeh and Professor Teofil Jesionowski for their valuable comments and suggestions on improving the design of the micro-sensor.

References

[1] E. Gallegos, A. Warren, E. Robles, E. Campoy, A. Calderon, M.G. Sainz, P. Bonilla, and O. Escolero, "The effects of wastewater irrigation on groundwater quality in Mexico", *Water Sci. Technol.* 40 (2), 45–52 (1999).

[2] Molecular Biology and Toxicology and Metals, eds. P.K. Zalups, J. Koropatnick, Taylor & Francis, New York, 2000.

[3] A. Jang, Y.W. Seo, and P.L. Bishop, "The removal of heavy metals in urban runoff by sorption on mulch", *Environ. Pollut.* 133, 117–128 (2005).

[4] M.F.M. Noh and I.E. Tothill, "Development and characterisation of disposable gold electrodes, and their use for lead (II) analysis", *Anal. Bioanal. Chem.* 386, 2095–2106 (2006).

[5] M.P. Waalkes, M. Anver, and B.A. Diwan, "Repeated cadmium exposures enhance the malignant progression of ensuing tumors in rats", *Toxicol. Sci.* 52, 154–161 (1999).

[6] D.G. Bostwick, H.B. Burke, D. Djakiew, S. Euling, S.M. Ho, J. Landolph, H. Morrison, B. Sonawane, T. Shifflett, D.J. Waters, and B. Timms, "Human prostate cancer risk factors", *Cancer: Cancer News* 101 (S10), 2371–2490 (2004).

[7] World Health Organization, Guidelines for drinking-water quality: first addendum to the fourth edition, 2017.

[8] T. Daşbaşı, Ş. Saçmacı, A. Ülgen, and Ş. Kartal, "A solid phase extraction procedure for the determination of Cd (II) and Pb (II) ions in food and water samples by flame atomic adsorption spectrometry", *Food Chem.* 174, 591–596 (2015).

[9] L.G. Danielsson, B. Magnusson, and S. Westerlund, "An improved metal extraction procedure for the determination of trace metals in sea water by atomic adsorption spectrometry with electrothermal atomization", *Anal. Chim. Acta* 98 (1), 47–57 (1978).

[10] M. Faraji, Y. Yamini, A. Saleh, M. Rezaee, M. Ghambarian, and R. Hassani, "A nanoparticle-based solid-phase extraction procedure followed by flow injection inductively coupled plasma-optical emission spectrometry to determine some heavy metal ions in water samples", *Anal. Chim. Acta* 659 (1-2), 172–177 (2010).

[11] L. Zhao, S. Zhong, K. Fang, Z. Qian, and J. Chen, "Determination of cadmium (II), cobalt (II), nickel (II), lead (II), zinc (II), and copper (II) in water samples using dual-cloud point extraction and inductively coupled plasma emission spectrometry", *J. Hazard. Mater.* 239, 206–212 (2012).

[12] Z. Chen, Z. Peng, J. Jiang, X. Zhang, G. Shen, and R. Yu, "An electrochemical amplification immunoassay using biocatalytic metal deposition coupled with anodic stripping voltammetric detection", *Sens. Actuators B: Chem.* 129, 146–151 (2008).

[13] W. Hu, H. Cai, J. Fu, P.Wang, and G. Yang, "Line-scanning LAPS array for measurement of heavy metal ions with microlens array based on MEMS", *Sens. Actuators B Chem.* 129, 397–403 (2008).

[14] S. Roy, A. Prasad, R. Tevatia, and R.F. Saraf, "Heavy metal ion detection on a microspot electrode using an optical electrochemical probe", *Electrochem. Commun.* 86, 94–98 (2018).

[15] A. Waheed, M. Mansha, and N. Ullah, "Nanomaterials-based electrochemical detection of heavy metals in water: Current status, challenges and future direction", *Trac-Trends Anal. Chem.* 105, 37–51 (2018).

[16] A. Moutcine and A. Chtaini, "Electrochemical determination of trace mercury in water sample using EDTA-CPE modified electrode", *Sensing and bio-sensing research* 17, 30–35 (2018).

[17] J. Chouler, M.D. Monti, W.J. Morgan, P.J. Cameron, and M. Di Lorenzo, "A photosynthetic toxicity biosensor for water", *Electrochim. Acta* 309, 392–401 (2019).

[18] P.S. Samendra, K. Masaaki, P.G. Charles, and L.P. Ian, "Rapid detection technologies for monitoring microorganisms in water", *Biosens. J.* 3 (109), 2 (2014).

[19] Y. Arntz, J.D. Seelig, H.P. Lang, J. Zhang, P. Hunziker, J.P. Ramseyer, E. Meyer, M. Hegner, and Ch. Gerber, "Label-free protein assay based on a nanomechanical cantilever array", *Nanotechnology* 14 (1), 86 (2002).

[20] G.E. Fantner, W. Schumann, R.J. Barbero, A. Deutschinger, V. Todorov, D.S. Gray, A.M. Belcher, I.W. Rangelow, and K. Youcef-Toumi. "Use of self-actuating and self-sensing cantilevers for imaging biological samples in fluid", *Nanotechnology* 20 (43) (2009).

[21] W. Zhang, and K.L. Turner, "Application of parametric resonance amplification in a single-crystal silicon micro-oscillator based mass sensor", *Sens. Actuators, A.* 122 (1), 23–30 (2005).

[22] P.S. Waggoner, and H.G. Craighead, "Micro-and nanomechanical sensors for environmental, chemical, and biological detection", *Lab Chip* 7 (10), 1238–1255 (2007).

[23] B. Ilic, D. Czaplewski, M. Zalalutdinov, H.G. Craighead, P. Neuzil, C. Campagnolo, and C. Batt, "Single cell detection with micromechanical oscillators", *J. Vac. Sci. Technol., B: Microelectron. Nanometer Struct.–Process., Meas., Phenom.* 19 (6), 2825–2828 (2001).

[24] P. Enoksson, G. Stemme, and E. Stemme, "A silicon resonant sensor structure for Coriolis mass-flow measurements", *J. Microelectromech. Syst.* 6(2), 119–125 (1997).

[25] K. Park, N. Kim, D.T. Morisette, N.R. Aluru, and R. Bashir, "Resonant MEMS mass sensors for measurement of microdroplet evaporation", *J. Microelectromech. Syst.* 21 (3), 702–711 (2012).

[26] S. Walczak, and M. Sibiński, "Flexible, textronic temperature sensors, based on carbon nanostructures", *Bull. Pol. Acad. Sci.: Tech. Sci.* 62 (4), 759–763 (2014).

[27] W.P. Jakubik, M. Urbańczyk, E. Maciak, and T. Pustelny, "Surface acoustic wave hydrogen gas sensor based on layered structure of palladium/metal-free phthalocyanine", *Bull. Pol. Acad. Sci.: Tech. Sci.* 56 (2), 133–138 (2008).

[28] A. Odabasic, I. Sestan, and S. Begic, "Biosensors for Determination of Heavy Metals in Waters", in *Environmental Biosensors*, 2019.

[29] K. Eom, H.S. Park, D.S. Yoon, and T. Kwon, "Nanomechanical resonators and their applications in biological/chemical detection: nanomechanics principles", *Phys. Rep*. 503 (4-5), 115–163 (2011).

[30] A. Gupta, D. Akin, and R. Bashir, "Detection of bacterial cells and antibodies using surface micromachined thin silicon cantilever resonators", *J. Vac. Sci. Technol., B: Microelectron. Nanometer Struct.–Process., Meas., Phenom*. 22 (6), 2785–2791 (2004).

[31] A. Gupta, D. Akin and R. Bashir, "Single virus particle mass detection using microresonators with nanoscale thickness", *Appl. Phys. Lett.* 84 (11), 1976–1978 (2004).

[32] K. Park, J. Jang, D. Irimia, J. Sturgis, J. Lee, J.P. Robinson, M. Toner, and R. Bashir, "Living cantilever arrays' for characterization of mass of single live cells in fluids", *Lab Chip* 8 (7), 1034–1041 (2008).

[33] G. Wu, H. Ji, K. Hansen, T. Thundat, R. Datar, R. Cote, M.F. Hagan, A.K. Chakraborty, and A. Majumdar, "Origin of nanomechanical cantilever motion generated from biomolecular interactions", *Proc. Natl. Acad. Sci*. 98 (4), 1560–1564 (2001).

[34] G. Wu, R.H. Datar, K.M. Hansen, T. Thundat, R.J. Cote, and A. Majumdar, "Bioassay of prostate-specific antigen (PSA) using microcantilevers", *Nat. Biotechnol.* 19 (9), 856 (2001).

[35] R.K. Gupta, S.V. Dobritsa, C.A. Stiles, M.E. Essington, Z. Liu, C.H. Chen, E.H. Serpersu and B.C. Mullin, "Metallohistins: A new class of plant metal-binding proteins", *J. Protein Chem*. 21 (8), 529–536 (2002).

[36] N. Verma and M. Singh, "Biosensors for heavy metals", *BioMetals* 18, 121–129 (2005).

[37] G.L. Turdean, "Design and Development of Biosensors for the Detection of Heavy Metal Toxicity", *Int. J. Electrochem.* 2011, 343125 (2011).

[38] G. Aragay, J. Pons, and A. Merkoçi, "Recent trends in macro-, micro-, and nanomaterial-based tools and strategies for heavy-metal detection", *Chem. Rev*. 111 (5), 3433–3458 (2011).

[39] T. Braun, V. Barwich, M.K. Ghatkesar, A.H. Bredekamp, C. Gerber, M. Hegner, and H.P. Lang, "Micromechanical mass sensors for biomolecular detection in a physiological environment", *Phys. Rev. E* 72 (3), 031907 (2005).

[40] M. Hara, D. Kashima, T. Horiike, and T. Kuboi, "Metal-binding characteristics of the protein which shows the highest histidine content in the Arabidopsis genome", *Plant Biotechnol. J.* 27(5), 475–480 (2010).

[41] O.A. Kapustina, "Degassing of liquids", *Physical Principles of Ultrasonic Technology*, IV, 422–427 (1970).

[42] C. Suman, R.K. Gupta, B.C. Mullin, and T. Thundat, "Detection of heavy metal ions using protein-functionalized microcantilever sensors", *Biosens. Bioelectron.* 19 (5), 411–416 (2003).

[43] J. Friend and L. Yeo, "Using laser Doppler vibrometry to measure capillary surface waves on fluid-fluid interfaces", *Biomicrofluidics* 4 (2), 026501 (2010).

[44] R. Longo, S. Vanlanduit, G. Arroud, and P. Guillaume, "Underwater acoustic wavefront visualization by scanning laser Doppler vibrometer for the characterization of focused ultrasonic transducers", *Sensors* 15 (8), 19925–19936 (2015).

[45] B. Bhushan, H. Fuchs, and S. Hosaka, *Applied Scanning Probe Methods I*, Springer Science & Business Media, 2014.

[46] R. Shabani, H. Hatami, F.G. Golzar, S. Tariverdilo, and G. Rezazadeh, "Coupled vibration of a cantilever micro-beam submerged in a bounded incompressible fluid domain", *Acta Mechanica* 224 (4), 841–850 (2013).

[47] A. Bouchaala, A.H. Nayfeh, and M.I. Younis, "Analytical study of the frequency shifts of micro and nano clamped–clamped beam resonators due to an added mass", *Meccanica* 52 (1-2), 333–348 (2017).

[48] Z. Rahimi, G. Rezazadeh, W. Sumelka, and X.J. Yang, "A study of critical point instability of micro and nano beams under a distributed variable-pressure force in the framework of the inhomogeneous non-linear nonlocal theory", *Arch. Mech.* 69 (6), 413–433 (2017).

[49] K. Ivaz, D. Abdollahi, and R. Shabani, "Analyzing Free Vibration of a Cantilever Microbeam Submerged in Fluid with Free Boundary Approach", *J. Appl. Fluid Mech*. 10 (6), 1593–1603 (2017).

[50] N. Sharafkhani, R. Shabani, S. Tariverdilo, and G. Rezazadeh, "Stability analysis and transient response of electrostatically actuated microbeam interacting with bounded compressible fluids", *J. Appl. Mech*. 80 (1), 011024 (2013).

[51] Z. Rahimi, G. Rezazadeh, and H. Sadeghian, "Study on the size dependent effective Young modulus by EPI method based on modified couple stress theory", *Microsyst. Technol*. 24, 2983–2989 (2018).

[52] Z. Rahimi, G. Rezazadeh, and W. Sumelka, "A non-local fractional stress–strain gradient theory", *Int. J. Mech. Mater. Des*. 16, 265–278 (2020).

[53] S.S. Rao, *Mechanical Vibration*, Prentice Hall, Pearson Education South Asia Pte Ltd., 2005.

[54] M. Marco, R. Battaglia, G. Ferrini, R. Puglisi, D. Balduzzi, and A. Galli, "Single microparticles mass measurement using an AFM cantilever resonator", arXiv preprint arXiv:1410.1953, (2014).

[55] C.C. Liang, C.C. Liao, Y.S. Tai, and W.H. Lai, "The free vibration analysis of submerged cantilever plates", *Ocean Eng.* 28 (9), 1225–1245 (2001).

[56] Y. Zhang and Y.P. Zhao, "Mass and force sensing of an adsorbate on a beam resonator sensor", *Sensors* 15(7), 14871–14886 (2015).